Vehicle

12 h				24 h				36 h				48 h			
–	+	++	+++	–	+	++	+++	–	+	++	+++	–	+	++	+++
0	6	0	0	6	0	0	0	0	6	0	0	6	0	0	0
6	0	0	0	6	0	0	0	6	0	0	0	6	0	0	0
6	0	0	0	6	0	0	0	6	0	0	0	6	0	0	0
6	0	0	0	6	0	0	0	6	0	0	0	6	0	0	0
(0)				(0)				(0)				(1)			
6	0	0	0	6	0	0	0	5	0	0	0				
6	0	0	0	6	0	0	0	6	0	0	0	5	0	0	0
6	0	0	0	6	0	0	0	6	0	0	0	6	0	0	0
6	0	0	0	0	0	0	0	6	0	0	0	6	0	0	0

SZ 200 mg/kg

12 h				24 h				36 h				48 h			
–	+	++	+++	–	+	++	+++	–	+	++	+++	–	+	++	+++
6	0	0	0	6	0	0	0	6	0	0	0	4	2	0	0
1	5	0	0	3	3	0	0	6	0	0	0	6	0	0	0
6	0	0	0	6	0	0	0	6	0	0	0	6	0	0	0
6	0	0	0	6	0	0	0	5	1	0	0	3	3	0	0
(0)				(0)				(0)				(1)			
6	0	0	0	6	0	0	0	4	2	0	0	1	2	2	0
6	0	0	0	6	0	0	0	4	2	0	0	2	3	0	0
0	0	0	6	0	0	0	6	3	3	0	0	6	0	0	0
6	0	0	0	6	0	0	0	1	5	0	0	1	5	0	0

Hematological findings (table 2): The values of RBC, Hb, Ht and neutrophil ratio in the SZ-treated mice significantly increased at 6 and 12 hours after the treatment. After that, they returned to normal values. The value of Ret in the SZ-treated mice significantly decreased at 36 and 48 hours after the treatment. No treatment-related changes were observed in other parameters.

Blood chemical findings (table 3): The serum glucose level in the SZ-treated group once decreased at 6 and 12 hours after the treatment and it became significantly higher than that in the vehicle control group at 36 and 48 hours after the treatment (fig. 1). On the other hand, the insulin level in the SZ-treated group was significantly higher than that in the vehicle control group at 6 and 12 hours after the treatment. It returned to normal level at 24 hours after the treatment and became lower level than that in the vehicle control group at 36 and 48 hours after the treatment (fig. 2).

The serum AST and ALT activities in the SZ-treated group were slightly higher than those in the vehicle control group from 6 to 36 hours after the treatment, but they returned to similar levels to those in the vehicle control

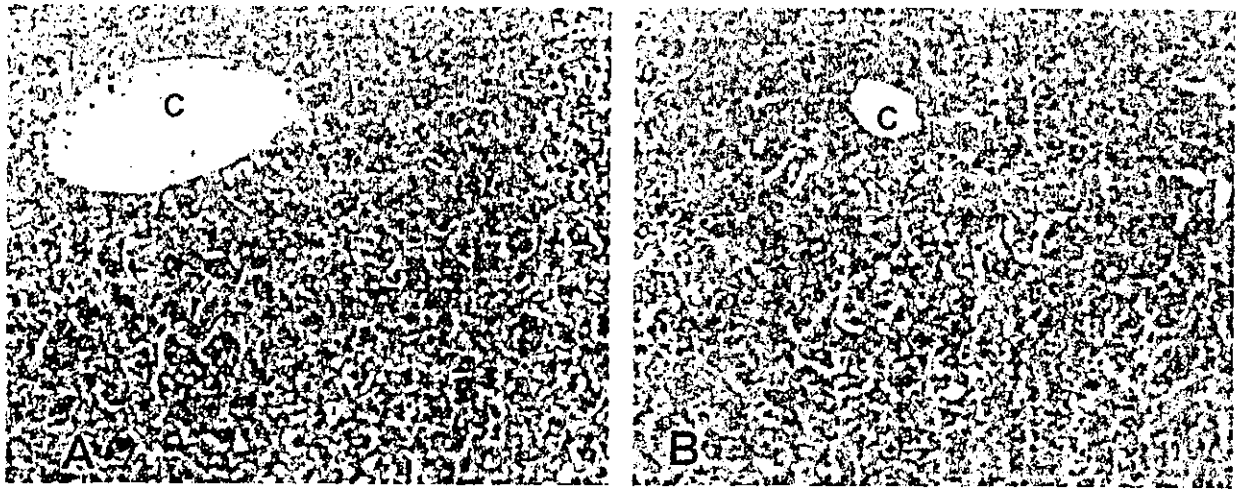

Fig. 7. Microphotographs of livers in mice treated with vehicle (A) or streptozotocin (B) at 48 hours after the treatment. Slight fatty change is observed in the streptozotocin-treated mouse (B). C: central vein. HE, ×200.

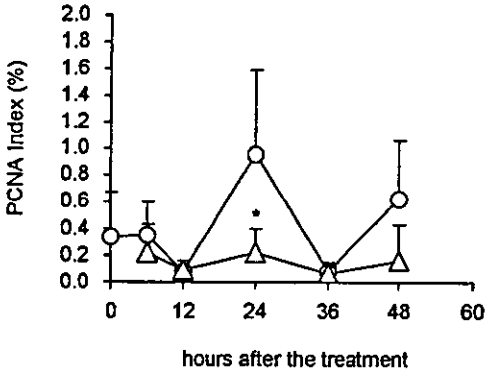

Fig. 8. Changes in PCNA index. ○: vehicle control group, △: SZ-treated group. Mean ± S.D. *: $p < 0.05$, Significantly different from the vehicle control group.

group at 48 hours after the treatment. The TG values at 6 and 12 hours after the treatment were higher in the SZ-treated group than in the vehicle control group. The PL and TCHO values were lower in the SZ-treated group than in the vehicle control group from 6 to 24 hours after the treatment. No treatment-related changes were observed in other parameters.

Liver biochemical findings (table 4): TBARS content in the SZ-treated group was higher than that in the vehicle control group from 6 to 24 hours after the treatment, which returned to similar level to that in the vehicle control group at 36 or 48 hours after the treatment (fig. 3). Phospholipid hydroperoxides (PE-OOH, PC-OOH) in the SZ-treated group were consistently higher than those in the vehicle control group (fig. 4).

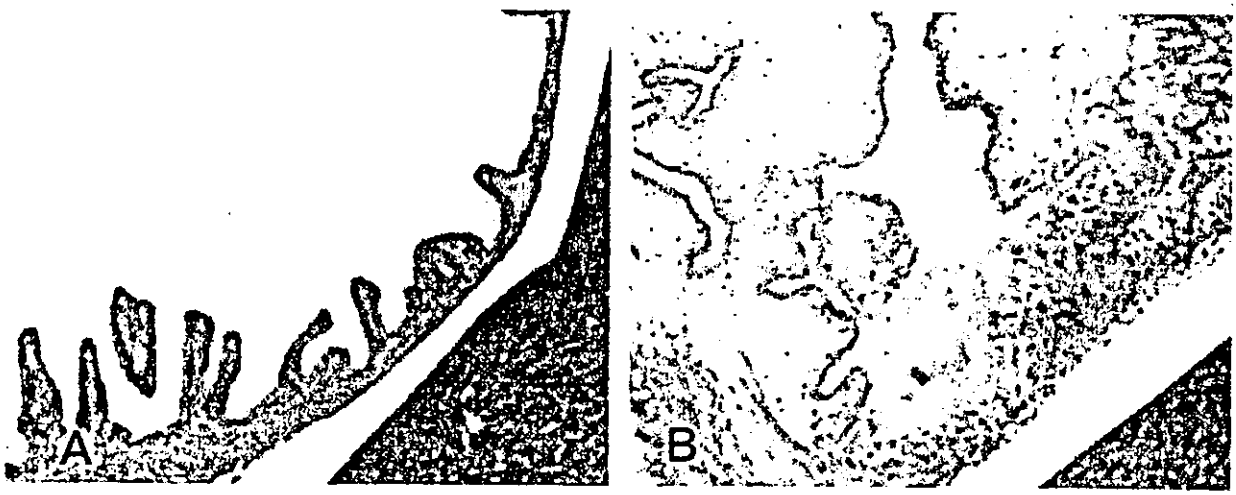

Fig. 9. Microphotographs of gallbladders in mice treated with vehicle (A) or streptozotocin (B) at 48 hours after the treatment. Note severe edema with neutrophil infiltration and ulcer of the gall bladder epithelium (B). HE, ×100.

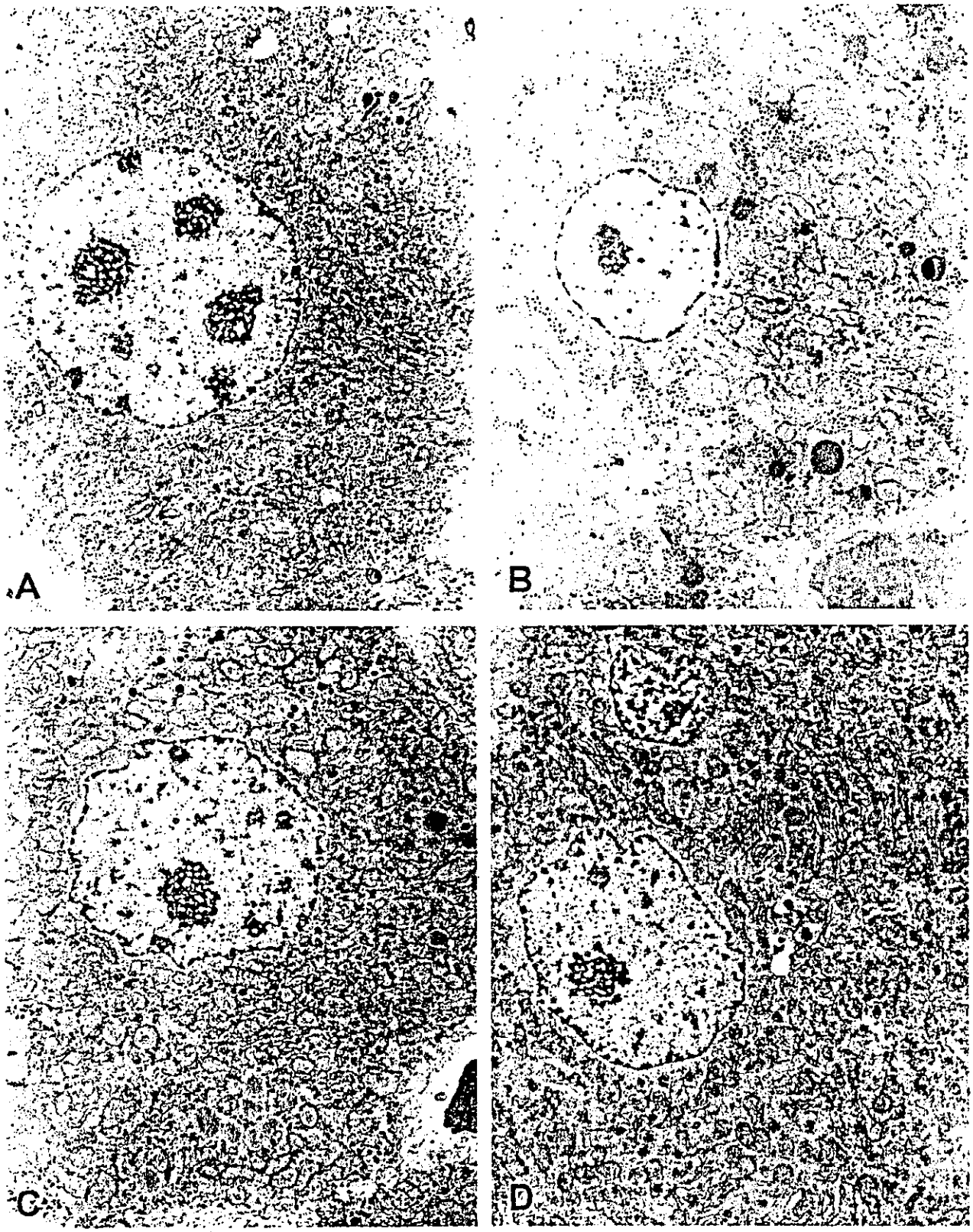

Fig. 10. Electron micrographs of hepatocytes in mice treated with vehicle (A) or streptozotocin (B, C, D). A, B: 6 hours after the treatment. C, D: 48 hours after the treatment. The hepatocytes from streptozotocin-treated mice show increased lipid droplets (B, C) and slight mitochondrial swelling (B–D). In addition, irregular arrangements of rough endoplasmic reticula and increased peroxisomes are observed at 48 hours after the treatment (C, D). ×4,200.

Light microscopic findings (table 5): In the pancreas of the SZ-treated group, severe pancreatic islet cell necrosis was observed from 6 to 24 hours after the treatment (fig. 5). After that, necrotic cells were removed from the islet and completely disappeared at 48 hours after the treatment. The size of the islet cells and the size of the islet itself were reduced at 36 and 48 hours after the treatment. No severe inflammation was observed throughout the experimental period.

At 6 hours after the treatment, cytoplasmic acidophilic granules, which are usually observed in normal hepatocytes, decreased in the hepatocytes of the SZ-treated mice. The cytoplasm of the hepatocytes of those mice looked somewhat pale and homogeneous (fig. 6). Glycogen area of hepatocytes in the vehicle control group varied under influence of circadian rhythm, which was large at morning (0, 24 and 48 hours after the treatment) and was small at night (12 and 36 hours after the treatment). In comparison, glycogen area in the SZ-treated group did not change with circadian rhythm and was greater than that of the vehicle control group from 6 to 24 hours after the treatment. One mouse at 36 hours after the treatment and 3 mice at 48 hours after the treatment showed slight fatty change of hepatocytes (fig. 7).

PCNA index also varied under influence of circadian rhythm in the vehicle control group, which was low at night (12 and 36 hours after the treatment) and was high at morning (24 and 48 hours after the treatment), although the index just before the treatment (untreated control; morning) was not as high as 24 and 48 hours after the treatment. On the other hand, the PCNA index in the SZ-treated mice did not change with circadian rhythm and was continuously low level throughout the experimental period (fig. 8).

In the gallbladder of the SZ-treated group, ulcer and submucosal edema were observed at 36 or 48 hours after the treatment (fig. 9).

Electron microscopic findings (fig. 10): At 6 hours after the treatment, the hepatocytes of the SZ-treated mice had greater amount of glycogens in comparison with those of the vehicle control mice. Lipid droplets also increased in number and size, and the layered structure of rough endoplasmic reticulum (rER) was not so parallel. In the midzonal area, mitochondria were somewhat swollen. At 48 hours after the treatment, like at 6 hours after the treatment, the hepatocytes of the SZ-treated mice showed increased lipid droplets and irregular arrangements of rERs. In addition, an increase in the number of peroxisomes was also observed especially in the midzonal and periportal areas. A part of the hepatocytes showed slight swelling and increased number of mitochondria.

Discussion

JUNOD et al. (1967) reported that the SZ-induced injury of the pancreatic beta cells occurred within 24 hours, and BROSKY and LOGOTHETOPOULOS (1969) reported that the injury started 2 to 4 hours after the administration. In this study, histopathological examinations revealed that severe pancreatic islet cell necrosis occurred at or before 6 hours after the treatment, and most of the necrotic cells were removed from the islet from 36 to 48 hours after the treatment without apparent inflammatory reaction. These histopathological changes of pancreatic islets corresponded well with the changes in serum insulin level, glucose level and glycogen area of hepatocytes. In the SZ-treated mice, the serum glucose level transiently decreased at 6 and 12 hours after the treatment, when the serum insulin level showed a transient increase. At 36 and 48 hours after the treatment, the serum insulin level reached lower level than normal one, and the serum glucose level became higher than that in the vehicle control group. These findings suggested that leaked insulin from necrotized β cells decreased the glucose level. After that, the glucose level increased probably due to the decrease in amount of insulin following β cell necrosis. The glycogen area of hepatocytes in mice treated with vehicle decreased at 12 and 36 hours after the treatment according to circadian rhythms. On the other hand, the increase in glycogen area was observed in the SZ-treated group at 6 and 12 hours after the treatment probably due to the high insulin level. Apparent depression of liver glycogens was not observed in the SZ-treated group even at 36 or 48 hours after the treatment, although serum insulin level decreased and serum glucose level increased at such time points. Increased glycogen content at 6 and 12 hours after the treatment should influenced the increase in liver weight. We do not know the reason why the kidney, heart, lung, and spleen weights decreased.

It has been well known that insulin also controls the lipid synthesis (ADACHI et al. 1965), and it is reported that type I diabetes causes an increase of serum lipids (BROWN et al. 1967). We also have shown increases in serum lipids (TG, TCHO and PL) at 4 to 12 weeks after SZ injection (KUME et al. 1994b). In this study, serum TG level slightly increased, although the TCHO and PL levels showed lower levels than those in the vehicle control group from 6 to 24 hours after the treatment. In addition, there was an increase in peroxisomes. These findings suggest that there may be some effects on the lipid metabolism even in the acute phase.

We have reported that oncocytic hepatocytes were observed in the SZ-induced diabetic mice (KUME et al. 1994b; ARMOCIDA et al. 1994) from 1 week after the SZ injection. Acidophilic and hypertrophic cells, which show a marked increase of mitochondria with intact morphology, have been called oncocytic cells or oxyphilic cells, and they are considered to be preneoplastic in nature (BANNASCH et al. 1985) or to indicate compensatory response to a local anoxia (LEFKOWITCH et al. 1980). In this study, mitochondrial swelling was observed at 6 hours after the treatment. At that time point, pancreatic islets were necrotized but the serum insulin level was

higher and glucose level was lower than those of the vehicle control mice. Therefore, it is reasonable to consider that the mitochondrial swelling did not occur as a secondary effect of diabetes but occurred by direct effect of SZ. The increase in number of mitochondria may be a compensatory response to the mitochondrial damage.

It is well known that lipid peroxides increase in many organs under diabetic condition (MATKOVICS et al. 1982; BASTER et al. 1998). In this study, TBARS were significantly higher at 6 hours after the treatment, and peroxidized phospholipids were also higher than those in the vehicle control group. After that, the TBARS level decreased and reached normal level at 36 or 48 hours after the treatment. These findings suggested that SZ itself caused a kind of oxidative stress and injured the cell membrane or cytoplasmic organelle including mitochondria at least within 6 hours after the treatment. Recently, IMAEDA et al. (2002a; 2002b) reported that SZ induced DNA damage in the liver and kidney of mice at 1 hour after the treatment, and that antioxidants such as Fluvastatin reduced the SZ-induced DNA damage. Oxidative stress induced by SZ could be related to the swelling of mitochondria at 6 hours after the treatment, and also might be related to the increase of mitochondria and nucleic atypia from 1 week after the treatment. Although increases in serum AST and ALT activities were not severe, these changes might suggest an alteration of cell membrane of hepatocytes in SZ-treatment mice, and it could be related to the oxidative stress.

SZ is one of the alkylating agents (BENNETT and PEGG 1981), and has the mitosis inhibitory action or inhibitory action of DNA synthesis (BOLZAN and BIANCHI 2002; CAPUCCI et al. 1995; BHUYAN et al. 1970). HERRMAN (1999) showed SZ itself did not inhibit the PCNA labeling index in hepatocytes of the SZ-treated rats at 30 or 90 days after the treatment. In our study, immunohistochemical examination with PCNA staining revealed that SZ could inhibit the proliferation of hepatocytes like other anticancer agents. In addition, a decrease in reticulocyte, which means a decrease in erythropoiesis, was also observed in this study. These effects on the cell proliferation could be related with the tumorigenic action of SZ (RAKIETEN et al. 1968; FELDMAN et al. 1977; OKAWA and DOI 1983). On the other hand, slight increases in RBC, Hb and Ht were observed at 6 and 12 hours after the SZ-treatment. It should have been a hemoconcentration rather than increase in hematopoiesis, although real reason is obscure. The reason why the neutrophil ratio increased is also obscure but it might be related to pancreatic and hepatic injury, although there were no apparent inflammatory reactions.

Ulcer and submucosal edema of the gallbladder were observed in the SZ-treated group at 36 or 48 hours after the treatment. Some researchers have supposed the increase in bile flow and the changes in the composition of the bile under the diabetic condition (SIOW et al. 1991; WATKINS and SANDERS 1995). CARNOVALE et al. (1984; 1986) reported that SZ decreased the bile flow, resulting in change in the bile composition within 24 hours after the SZ-treatment. However, to the best of our knowledge, this is the first report that the acute gallbladder injury was induced by SZ-treatment. SZ concentrated at liver, kidney and pancreas, but the main elimination route of the drug is urinary excretion (KARUNANAYAKE et al. 1974, 1975). The drug concentration in the bile was considered not to be high level. Although the detailed mechanisms of this injury are obscure, one possibility might be changes in the composition of bile salt, and, in addition, the gallbladder epithelium might be highly sensitive to SZ. Anyhow, the injury of the gallbladder or bile duct epithelium is thought to be related to the bile duct hyperplasia or cholangiocarcinoma induced by SZ (OKAWA and DOI 1983; KUME et al. 1994).

In conclusion, this study revealed the characteristics of hepatic changes in the acute phase of SZ-induced diabetes in mice. SZ induced lipid peroxidation, mitochondrial swelling, peroxisome proliferation and inhibition of hepatocyte proliferation within 24 hours after the treatment, when hyperglycemia was not induced yet. Injury of gallbladder mucosa was also induced at 36 or 48 hours after the treatment. These findings were considered to be related with fatty change, mitochondrial proliferation, atypia of nuclei in hepatocytes observed in the subacute phase of SZ-induced diabetes (KUME et al. 1994b; DOI et al. 1997), or with bile duct hyperplasia (KUME et al. 1994a) and tumorigenic action of SZ (RAKIETEN et al. 1968; FELDMAN et al. 1977; OKAWA and DOI 1983).

Acknowledgement: We thank Mr. S. KURABE, Ms. M. KURABE, Ms. E. OHTSUKA, Ms. N. SHIMAZU, Ms. M. TAKAHASHI and other members of our laboratory for their technical assistance. We also thank Dr. Y. OHMACHI for earlier contribution to this work.

Reference

ADACHI K, INOUE H, TANIOKA H, TAKEDA Y: The biochemistry of animal cells. 3. Effect of insulin on lipid synthesis in dispersed rat liver cells. J Biochem 1965; **58**: 68–72.

ARMOCIDA AD, ITAGAKI S, KUME E, DOI K: Hepatic lesion in streptozotocin (SZ)-induced diabetic mice. J Toxicol Pathol 1994; **7**: 87–90.

BANNASH P, ZERBAN H, HACKER HJ: Foci of altered hepatocytes, rat. In: Digestive system (JONES TC, MOHE U, HUNT RD, eds), pp 10–30. Berlin: Springer-Verlag Berlin, 1985.

BASTAR I, SECKIN S, UYSAL M, AYKAC-TOKER G: Effect of streptozotocin on glutathione and lipid peroxide levels in various tissues of rats. Res Commun Mol Pathol Pharmacol 1998; **102**: 265–272.

BENNETT RA, PEGG AE: Alkylation of DNA in rat tissues following administration of streptozotocin. Cancer Res 1981; **41**: 2786–2790.

BERMAN LD, HAYES JA, SIBAY TM: Effect of streptozotocin in the Chinese hamster (Cricetulus griseus). J Natl Cancer Inst 1973; **51**: 1287–1294.

BHUYAN BK: The action of streptozotocin on mammalian cells. Cancer Res 1970; **30**: 2017–2023.

BOLZAN AD, BIANCHI MS: Chromosomal response of human lymphocytes to streptozotocin. Mutation Res 2002; **503**: 63–68.

BROSKY G, LOGOTHETOPOULOS J: Streptozotocin diabetes in the mouse and guinea pig. Diabetes 1969; **18**: 606–611.

BROWN DF: Triglyceride metabolism in the alloxan-diabetic rat. Diabetes 1967; **16**: 90–95.

CAPUCCI MS, HOFFMANN ME, DE GROOT A, NATARAJAN AT: Streptozotocin-induced toxicity in CHO-9 and V79 cells. Environ Mol Mutagen 1995; **26**: 72–78.

CARNOVALE CE, RODRIGUEZ GARAY EA: Reversible impairment of hepatobiliary function induced by streptozotocin in the rat. Experientia 1984; **40**: 248–250.

CARNOVALE CE, MARINELLI RA, RODRIGUEZ GARAY EA: Bile flow decrease and altered bile composition in streptozotocin-treated rats. Biochem Pharmacol 1986; **35**: 2625–2628.

DOI K, YAMANOUCHI J, KUME E, YASOSHIMA A: Morphologic changes in hepatocyte nuclei of streptozotocin (SZ)-induced diabetic mice. Exp Toxic Pathol 1997; **49**: 295–299.

FELDMAN S, SCHARP D, HIRSHBERG G, DODI G, BALLINGER W, LACY P: Streptozotocin-induced liver tumors. Transplantation 1977; **24**: 152–154.

HERRMAN CE, SANDERS RA, KLAUNIG JE, SCHWARZ LR, WATKINS JB 3rd.: Decreased apoptosis as a mechanism for hepatomegaly in streptozotocin-induced diabetic rats. Toxicol Sci 1999; **50**: 146–151.

IMAEDA A, KANEKO T, AOKI T, KONDO Y, NAGASE H: DNA damage and the effect of antioxidants in streptozotocin-treated mice. Food Chem Toxicol 2002; **40**: 979–987.

IMAEDA A, KANEKO T, AOKI T, KONDO Y, NAKAMURA N, NAGASE H, YOSHIKAWA T: Antioxidative effects of fluvastatin and its metabolites against DNA damage in streptozotocin-treated mice. Food Chem Toxicol 2002; **40**: 1415–1422.

JUNOD A, LAMBERT AE, ORCI L, PICTET R, GONET AE, RENOLD AE: Studies of the diabetogenic action of streptozotocin. Proc Soc Exp Biol Med 1967; **126**: 201–205.

KARUNANAYAKE EH, HEARSE DJ, MELLOWS G: The synthesis of [14C] streptozotocin and its distribution and excretion in the rat. Biochem J 1974; **142**: 673–683.

KARUNANAYAKE EH, HEARSE DJ, MELLOWS G: The metabolic fate and elimination of streptozotocin. Biochem Soc Trans1975; **3**: 410–414.

KUME E, DOI C, ITAGAKI S, NAGASHIMA Y, DOI K: Glomerular lesions in unilateral nephrectomized and diabetic (UN-D) mice. J Vet Med Sci 1992; **54**: 1085–1090.

KUME E, ITAGAKI S, DOI K: Cytomegalic hepatocytes and bile duct hyperplasia in streptozotocin-induced diabetic mice. J Toxicol Pathol 1994a; **7**: 261–265.

KUME E, OHMACHI Y, ITAGAKI S, TAMURA K, DOI K: Hepatic changes of mice in the subacute phase of streptozotocin (SZ)-induced diabetes. Exp Toxic Pathol 1994b; **46**: 368–374.

LEFKOWITCH JH, ARBORGH BA, SCHEUER PJ: Oxyphilic granular hepatocytes. Mitochondrion-rich liver cells in hepatic disease. Am J Clin Pathol 1980; **74**: 432–441.

LEVINE BS, HENRY MC, PORT CD, ROSEN E: Toxicologic evaluation of streptozotocin (NSC 85998) in mice, dogs and monkeys. Drug and Chem Toxicol 1980; **3**: 201–212.

MATKOVICS B, VARGA SI, SZABO L, WITAS H: The effect of diabetes on the activities of the peroxide metabolism enzymes. Horm Metab Res 1982; **14**: 77–79.

MATSUKI N, TAMURA S, ONO K, WATARI T, GOTTSUKA R, TAKAGI S, HASEGAWA A: The high-performance liquid chromatographic analysis for the peroxidized phospholipids in equine erythrocytes and skeletal muscle. J Vet Med Sci 1991; **53**: 717–719.

OKAWA H, DOI K: Neoplastic lesions in streptozotocin-treated rats. Exp Anim 1983; **32**: 77–84.

RAKIETEN N, GORDON BS, COONEY DA, DAVIS RD, SCHEIN PS: Renal tumorigenic action of streptozotocin (NSC-85998) in rats. Cancer Chemother Rep 1968; **52**: 563–567.

SCHEIN PS, O'CONNELL MJ, BLOM J, HUBBARD S, MAGRATH IT, BERGEVIN P, WIERNIK PH, ZIEGLER JL, DEVITA VT: Clinical antitumor activity and toxicity of streptozotocin (NSC-85998). Cancer 1974; **34**: 993–1000.

SCHMEDES A, HØLMER G: A new thiobarbituric acid (TBA) method for determining free malondialdehyde (MDA) and hydroperoxides selectively as a measure of liquid peroxidation. J Am Oil Chem Soc 1989; **66**: 813–817.

SIBAY TM, HAUSLER HR, HAYES JA: The study and effect of streptozotocin (NSC-37917) rendered diabetic chinese hamsters. Annals Ophthalmol 1971; **3**: 596–601.

SIOW Y, SCHURR A, VITALE GC: Diabetes-induced bile acid composition changes in rat bile determined by high performance liquid chromatography. Life Sci 1991; **49**: 1301–1308.

STEFFES MW, MAUER SM: Diabetic glomerulopathy in man and experimental animal models. Int Rev Exp Pathol 1984; **26**: 147–175.

VAVRA JJ, DEBOER C, DIETZ A, HANKA LJ, SOKOLSKI WT: Streptozotocin, a new antibacterial antibiotic. Antibiotics anual 1959–1960: 230–235.

WATKINS JB 3rd, SANDERS RA: Diabetes mellitus-induced alterations of hepatobiliary function. Pharmacol Rev 1995; **47**: 1–23.

WEISS RB: Streptozocin: a review of its pharmacology, efficacy, and toxicity. Cancer Chemother Rep 1982; **66**: 427–438.

WHITE FR: Streptozotocin. Cancer Chemother Rep 1963; **30**: 49–53.

Available online at www.sciencedirect.com
SCIENCE DIRECT®
Biochemical and Biophysical Research Communications 313 (2004) 789–793
BBRC
www.elsevier.com/locate/ybbrc

Novel single nucleotide polymorphisms of organic cation transporter 1 (*SLC22A1*) affecting transport functions

Takeshi Sakata,[a,b] Naohiko Anzai,[a] Ho Jung Shin,[a] Rie Noshiro,[a,b] Taku Hirata,[a] Hirokazu Yokoyama,[a] Yoshikatsu Kanai,[a] and Hitoshi Endou[a,*]

[a] *Department of Pharmacology and Toxicology, Kyorin University School of Medicine, 6-20-2 Shinkawa, Mitaka-shi, Tokyo 181-8611, Japan*
[b] *Kobuchisawa Research Laboratories, Fuji Biomedix Co. Ltd., 10221 Kobuchisawa-cho, Kitakoma-gun, Yamanashi 408-0044, Japan*

Received 5 November 2003

Abstract

Organic cation transporter OCT1 (*SLC22A1*) plays an essential role in absorption, distribution, and excretion of various xenobiotics including therapeutically important drugs. In the present study, we analyzed the functional properties of the single nucleotide polymorphisms (SNPs) in *SLC22A1* gene found in Japanese control individuals. Four mutations resulting in the amino acid changes (F160L, P283L, R287G, and P341L) were functionally characterized in *Xenopus* oocyte expression system. Two new SNPs, identified in Japanese population, P283L and R287G exhibited no uptake of both [^{14}C]TEA and [^{3}H]MPP^{+}, although their protein expressions were detected in the plasma membrane of the oocytes injected with their cRNAs. Uptake of [^{14}C]TEA by P341L was reduced to 65.1% compared to wild type, whereas F160L showed no significant change in its transport activity. This study suggests that the newly found OCT1 variants will contribute to inter-individual variations leading to the differences in cationic drug disposition and perhaps certain disease processes.
Published by Elsevier Inc.

Keywords: Organic cation transporter; Single nucleotide polymorphisms; Tetraethylammonium; MPP^{+}

It has long been recognized that genetic variations in drug metabolizing enzymes underlie the inter-individual differences in drug response [1]. Certain single nucleotide polymorphisms (SNPs) in cytochrome P450 systems, such as CYP2D6, are well known to be related to altered drug metabolism, unexpected drug effect, and alterations of the clinical response and frequency of side effects [2,3]. Molecular studies in pharmacogenetics have now been extended to numerous other human genes including those for several drug transport systems. For example, SNPs in the ABC (ATP-binding cassette) transporter *MDR1* gene were reported to influence the disposition of digoxin [4] and fexofenadine [5]. Furthermore, SNPs in the SLC (solute carrier) transporter OATP-C and OATP-B gene result in the decrease of drug transport activity [6,7].

Organic cation transporters (OCTs) mediate electrogenic transport of small organic cations with different molecular structures, independently of sodium gradient [8]. These organic cations include clinically used drugs (e.g., metformin), endogenous compounds (e.g., dopamin), as well as toxic substances (e.g., MPP^{+}). Human OCT1 (*SLC22A1*), expressed primarily in the liver, plays a fundamental role in the cellular uptake and elimination of various cationic substrates including therapeutically important agents [9,10]. Recently, several functionally relevant mutations of *SLC22A1* were identified by two groups. Kerb et al. [11] found that uptakes of [^{3}H]MPP^{+} by R61C, C88R, and G401S were reduced compared to that of wild-type OCT1 and Shu et al. [12] reported that R61C, P341L, G220V, G401S, and G465R showed reduced function, whereas S14F exhibited increased function.

In this report, we analyzed the functional properties of the OCT1 variants found in Japanese populations (an online database of Japanese single nucleotide polymorphisms [13] at http://snp.ims.u-tokyo.ac.jp) by using

* Corresponding author. Fax: +81-422-79-1321.
E-mail address: endouh@kyorin-u.ac.jp (H. Endou).

0006-291X/$ - see front matter. Published by Elsevier Inc.
doi:10.1016/j.bbrc.2003.11.175

Xenopus oocyte expression system. We demonstrated that two new variants are associated with severe decrease in transport activity.

Materials and methods

Materials. [^{14}C]TEA (2.05 GBq/mmol) and [^{3}H]MPP^{+} (2.96 TBq/mmol) were purchased from American Radiolabeled Chemicals (USA). All other chemicals and reagents were of analytical grade. Rabbit polyclonal antibodies were raised against a synthetic carboxyl-terminal peptide of human OCT1, ENLGRKAKPKENC, as reported previously [14].

Isolation of human OCT1 cDNA. Specific PCR primers were designed based on the nucleotide sequence for human OCT1 (GenBank Accession Nos. U77086 and NM_003057) [9]: forward primer, 5′-ATG AAG TGG ACT GGA ACC AGA C-3′ and reverse primer, 5′-TTT GTG ATA ACA GCC ACC GAG G-3′. One microgram of poly(A)$^{+}$ RNA from human liver (purchased from Clontech) was reverse-transcribed and used as a template for subsequent PCR. A PCR product was labeled with [^{32}P]dCTP by random priming method (T7 Quick Prime Kit, Amersham–Pharmacia Biotech) and used for the cDNA library screening. A nondirectional cDNA library was prepared from human liver poly(A)$^{+}$ RNA using the Superscript Choice system (Life Technologies) and screened as described previously [14]. The isolated cDNAs were subcloned into pcDNA3.1(−) (Invitrogen) and completely sequenced in both strands using ABI 3100 Genetic Analyzer (Applied Biosystems).

Site-directed mutagenesis. The nucleotide sequences of the full-length clones we obtained were identical to those reported previously [9] except for one nucleotide change which alters Phe^{160} to Leu. Thus, first we introduced point mutation (Leu to Phe) to this clone in order to prepare the wild-type OCT1. Then, we performed second site-directed mutagenesis to generate three OCT1 variants (P283L, R287G, and P341L) by using wild type clone as a template. The QuickChange Site-Directed Mutagenesis Kit (Stratagene) was used to introduce point mutations into OCT1 cDNA in the expression vector according to the instructions. Complementary oligonucleotides used for mutagenesis are described in Table 1. All the final sequences were confirmed by DNA sequencing.

cRNA synthesis and transport measurements. cRNA synthesis and uptake experiment were performed as described previously [14]. The capped cRNAs were synthesized in vitro using T7 RNA polymerase from the plasmid DNAs linearized with *Xba*I. Defolliculated oocytes were injected with 10 ng of the capped cRNA and incubated in Barth's solution (88 mM NaCl, 1 mM KCl, 0.33 mM $Ca(NO_3)_2$, 0.4 mM $CaCl_2$, 0.8 mM $MgSO_4$, 2.4 mM $NaHCO_3$, and 10 mM Hepes) containing 50 μg/ml gentamicin and 2.5 mM pyruvate, pH 7.4, at 18 °C. After incubation for 2–3 days, uptake experiments were performed at room temperature in ND96 solution (96 mM NaCl, 2 mM KCl, 1.8 mM $CaCl_2$, 1 mM $MgCl_2$, and 5 mM Hepes, pH 7.4). The uptake reaction was initiated by replacing ND96 solution with that containing a radiolabeled ligand and terminated by the addition of ice-cold ND96 solution and following five times washes after 1 h of incubation. Oocytes were, then, solubilized with 10% SDS and analyzed by scintillation counting.

To estimate kinetic parameters for the uptake of TEA via wild-type OCT1 and mutants, the OCT1-mediated transport rates were obtained by subtracting the transport rate of noninjected oocytes from that of OCT1-expressing oocytes, and fit to the Michaelis–Menten curve by an iterative nonlinear least squares method using a MULTI program using the Damping Gauss Newton Method algorithm. The fitted line was converted to the *V/S* versus V form (Eadie–Hofstee plot) to calculate K_m and V_{max} values.

Immunofluorescent analysis. Xenopus laevis oocytes were injected with cRNAs for wild-type OCT1 and mutants. Two days after injection, the oocytes were fixed with paraformaldehyde and incubated with the anti-OCT1 antibody (1:100), followed by Alexa594-labeled goat anti-rabbit immunoglobulin-(IgG) (Wako; diluted 1:200). The sections were examined under an Olympus BX60 microscope equipped with BX-FLA unit (Olympus).

Results and discussion

Polymorphisms in OCT1 in Japanese population

In JSNP database, we found four nonsynonymous nucleotide polymorphisms of OCT1: F160L (JSNP ID: ssj0008476), P283L (ssj0005319), R287G (ssj0005320), and P341L (ssj0008480). SNPs F160L and P341L were same as those reported previously for American population [11,12], while SNPs P283L and R287G are only found in Japanese population. As shown in Fig. 1, F160 is located in the middle of the second transmembrane

Table 1
Summary of nonsynonymous polymorphisms in hOCT1 in Japanese

JSNP ID	Sequence	Protein residue	Oligonucleotides for mutagenesis	Scoring systems	
				Grantham	BLOSUM62
ssj0008476	cgggc ttctt C/G ttigg ctctc	F160L	Forward: 5′-gcgggcttgttgtttggctctctcg-3′[a] Reverse: 5′-cgagagagccaaagaagaagcccg-3′[a]	22	0
ssj0005319	aggtg tgtgc C/T ggagt cccct	P283L	Forward: 5′-ctggtgtgtgctggagtccccctcgg-3′ Reverse: 5′-ccgaggggactccagcacacacca-3′	98	−3
ssj0005320	ggagt cccct C/G ggtgg ctgtt	R287G	Forward: 5′-cggagtcccctgggtggctgttatc-3′ Reverse: 5′-gataacagccacccaggggactccg-3′	125	−2
ssj0008480	ttccg cacgc C/T gcgcc tgagg	P341L	Forward: 5′-gttccgcacgctgcgcctgaggaag-3′ Reverse: 5′-cttcctcaggcgcagcgtgcggaac-3′	98	−2

[a] These primers were used for hOCT1-WT creation.

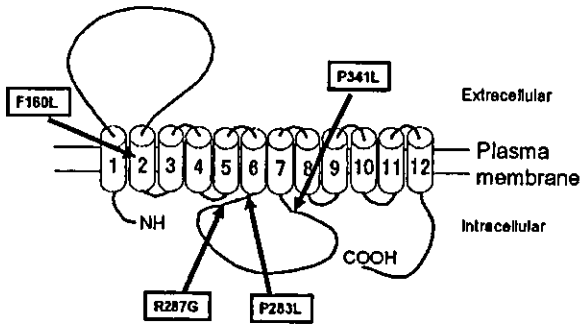

Fig. 1. Schematic representation of OCT1. Transmembrane topology is based on the previous report. Nonsynonymous nucleotide substitutions are indicated by arrows.

domain (TMD): P283 and R287 are at the 5′-end of long intracellular loop between 6th and 7th TMDs: P341 is located near the 3′-end of the long intracellular loop. F160 is conserved for both OCT1 and OCT2, and P341 is conserved among OCT1–3. In contrast, both P283 and R287 are conserved for OCT1–3 as well as OCTN1–2. They are in the conserved motif (P–E–S–P–R–X–L) of the major facilitator superfamily (MFS) as Burckhardt and Wolff mentioned before [15]. Particularly, R287 is conserved not only in OCT family but also in OAT family. These findings suggest the fundamental role of these two residues for their transport activities.

Functional analysis of OCT1 variants in Xenopus oocytes

To examine whether OCT1 polymorphisms found in Japanese population affect functional activities, we constructed site-directed mutants and expressed them in *Xenopus* oocytes. As Fig. 2 shows, the uptakes of [^{14}C]TEA and [^{3}H]MPP^{+} were eliminated for P283L and R287G. In contrast, P341L exhibited [^{14}C]TEA uptake partly reduced compared with wild-type OCT1. F160L showed no significant change. The results of F160L and P341L were consistent with the recent reports [11,12]. For F160L and P341L variants, we performed kinetic analysis for [^{14}C]TEA uptake (Fig. 3). The K_m values for wild type, F160L, and P341L were 192.0, 205.3, and 121.0 μM, respectively, and the V_{max} values for wild type, F160L, and P341L were 4.13, 4.42, and 2.33 pmol/h/oocyte, respectively. The values for wild type and F160L were similar to the previous report using *Xenopus* oocyte system [11,12].

Surface expression of hOCT1 variants at the plasma membrane of oocytes

Plasma membrane localizations of OCT1 variants were examined by immunofluorescent analysis. Figs. 4B–F shows the staining of OCT1 proteins in oocytes injected with cRNAs for OCT1 variants. Wild type and mutant OCT1 proteins were largely localized in the

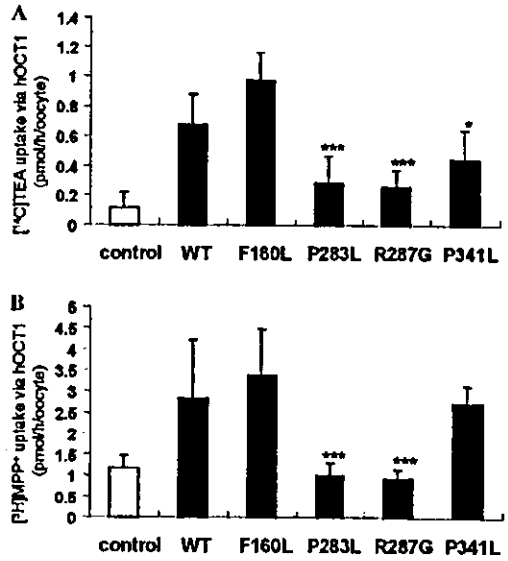

Fig. 2. Functional characterization of OCT1 variants. (A) The uptake of [^{14}C]TEA (10 μM) at 60 min in noninjected and OCT1 wild type and mutant cRNA-injected oocytes was measured on day 2 after injection is described in Materials and methods. (B) Functional characterization of OCT1 variants. The uptake of [^{3}H]MPP^{+} (10 μM) at 60 min in noninjected and OCT1 wild type and mutants cRNA-injected oocytes was measured on day 2 after injection is described in materials and methods. The data represent means ± SD for 7–9 oocytes. $^{*}p < 0.05$, $^{***}p < 0.001$ relative to wild type (WT) using Student's t test.

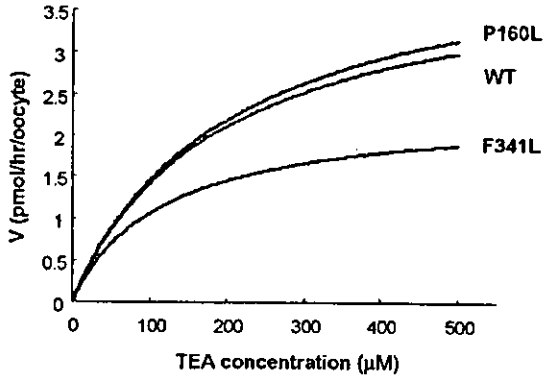

Fig. 3. Kinetic analysis of OCT1 variants. Concentration dependence of [^{14}C]TEA uptake in OCT1 wild type and variants (F160L, P341L) expressing oocytes. The uptakes of [^{14}C]TEA were measured at the concentration indicated after incubation for 1 h (n = 8–10). OCT1-mediated transport was obtained by subtracting the transport rates in noninjected oocytes from those in OCT1-expressing oocytes.

plasma membrane, confirming that altered transport activities are not due to the decreased expression levels of OCT1 protein at the plasma membranes, but due to the decreased functional activity of transporter per se.

Prediction of functional alterations in OCT1 variants

Recently, many large-scale screenings were carried out to identify genetic variants that affect disease

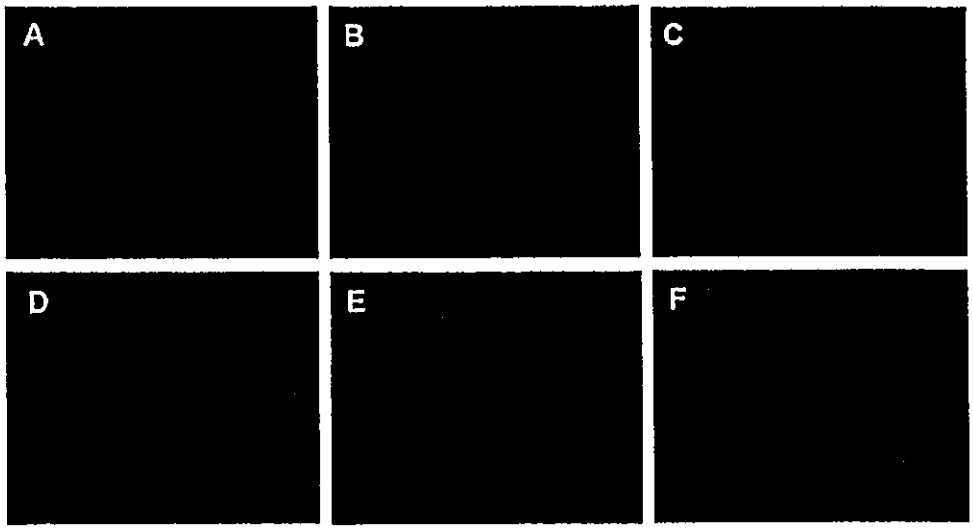

Fig. 4. Surface expression of OCT1 wild type and its variants at the plasma membrane of *Xenopus* oocytes. Immunodetection with a specific antibody raised against the C terminus of OCT1 showed that the wild type (B) as well as four mutant proteins [(C) F160L, (D) P283L, (E) R287G, and (F) P341L] are expressed at the plasma membrane. This antibody did not exhibit specific staining in the control oocytes injected water instead of cRNAs (A).

susceptibility and drug response. To determine which of the variants affect function and contribute to altered phenotype is the next important issue. Shu et al. [12] evaluated their 15 protein-altering variants of OCT1 by using amino acid scoring systems (chemical changes and evolutionary conservation). They reported that the variants with decreased function had larger chemical changes (greater Grantham values) than variants that did not reduce function and they also observed that the BLOSUM62 values for the decreased-function variants were significantly more negative (evolutionary unfavorable) than values for the variants that retained function. Grantham value is the criterion to assess chemical relatedness [16] and is expected to be useful for predicting deleterious function. BLOSUM62, an amino acid substitution matrix, is derived from amino acid changes in an unselected protein set [17] and has been used to infer protein function.

Following the report of Shu et al., we attempted to evaluate the changes in our OCT1 variants by chemical changes (Grantham value) and by amino acid substitution scoring matrices (BLOSUM62). As shown in Table 1, two completely nonfunctional variants had Grantham values of 98 (P283L) and 125 (R287G), indicating that radical changes are responsible for their reduced function. These two variants had negative BLOSUM62 scores; −3 (F283L) and −2 (R287G), demonstrating that this score was also useful for predicting protein function in our cases.

Variations of OCT1 and functional importance

Until now, there is no report on the phenotypic differences suspected to be due to the OCT1 polymorphism. However, our finding as well as those of two recent reports [11,12] may indicate that these mutations are associated with impaired OCT1 transport function and influence pharmacokinetics of OCT1 substrates. Jonker et al. [18] reported that Oct1 knockout mice exhibit decreased liver accumulation of the anti-cancer drug metaiodobenzylguanidine (MIBG) and the neurotoxin MPP^+. Wang et al. [19] also demonstrated the reduced distribution of the anti-diabetic drug metformin to the liver in *Oct1*$^{-/-}$ mice. Thus, it is interesting to know whether the similar effects are observed in the individuals with altered OCT1 function. In addition, it is well understood that the frequency of SNPs sometime varies among races, as has been reported for metabolic enzymes [20] and the transporter MDR1 [5]. To date, there is no report about the phenotype with reduced excretion of some cationic drugs in Japanese population. It was, however, indicated that the polymorphism of hepatic *N*-acetyltransferase NAT2*4, which is highly frequent in Japanese, correlates with acetylation of anti-arrhythmic drug procainamide, one of the OCT1 substrates [21]. The procainamide-induced systemic lupus erythematosus-like syndrome is closely related to the slow acetylator phenotype [22,23]. Since membrane transporters and metabolic enzymes are both involved in hepatic clearance of drugs, alteration of drug transport activities in the liver due to the genetic polymorphism could also have an important influence on drug effect and side effects because of reduced excretion. Therefore, further understanding of the relation between certain cationic drug dispositions and race-specific OCT1 variations will not only contribute to inter-individual variations but also will lead to the understanding of the differences across different populations in cationic drug disposition and perhaps certain disease processes.

Acknowledgments

The anti-hOCT1 polyclonal antibody was supplied by Transgenic Inc. Kumamoto, Japan. This work was supported in part by grants from the Ministry of Education Science, Sports, Culture and Technology of Japan, and from the Japanese Society for the Promotion of Science (JSPS). This work was performed in collaboration with PharmaSNP consortium.

References

[1] M. Ingelman-Sundberg, M. Oscarson, R.A. McLellan, Polymorphic human cytochrome P450 enzymes: an opportunity for individualized drug treatment, Trends Pharmacol. Sci. 20 (1999) 342–349.

[2] W.E. Evans, M.V. Relling, Pharmacogenomics: translating functional genomics into rational therapeutics, Science 286 (1999) 487–491.

[3] U.A. Meyer, U.M. Zanger, Molecular mechanisms of genetic polymorphisms of drug metabolism, Annu. Rev. Pharmacol. Toxicol. 37 (1997) 269–296.

[4] S. Hoffmeyer, O. Burk, O. von Richter, H.P. Arnold, J. Brockmoller, A. Johne, I. Cascorbi, T. Gerloff, I. Roots, M. Eichelbaum, U. Brinkman, Functional polymorphisms of the human multidrug-resistance gene: multiple sequence variations and correlation of one allele with *P*-glycoprotein expression and activity in vivo, Proc. Natl. Acad. Sci. 97 (2000) 3473–3478.

[5] R.B. Kim, B.F. Leake, E.F. Choo, G.K. Dresser, S.V. Kubba, U.I. Schwartz, A. Taylor, H.-G. Xie, J. McKinsey, S. Zhou, L. Lu-Bin, J.D. Schuetz, E.G. Schuetz, G.R. Wilkinson, Identification of functional variant MDR1 alleles among European American and African American, Clin. Pharmacol. Ther. 70 (2001) 189–199.

[6] R.G. Tirona, B.F. Leake, G. Merino, R.B. Kim, Polymorphisms in *OATP-C*. Identification of multiple allelic variants associated with altered transport activity among European- and African-Americans, J. Biol. Chem. 276 (2001) 35669–35675.

[7] T. Nozawa, M. Nakajima, I. Tamai, K. Noda, J.-I. Nezu, Y. Sai, A. Tsuji, T. Yokoi, Genetic polymorphisms of human organic anion transporters OATP-C (SLC21A6) and OATP-B (SLC21A9): allele frequencies in the Japanese population and functional analysis, J. Phamacol. Exp. Ther. 302 (2002) 804–813.

[8] H. Koepsell, Organic cation transporters in intestine, kidney, liver, and brain, Annu. Rev. Physiol. 60 (1998) 243–266.

[9] L. Zhang, M.J. Dresser, A.T. Gray, S.C. Yost, S. Terashita, K.M. Giacomini, Cloning and functional expression of a human liver organic cation transporter, Mol. Pharmacol. 51 (1997) 913–921.

[10] V. Gorboulev, J.C. Ulzheimer, A. Akhoundova, I. Ulzheimer-Teuber, U. Karbach, S. Quester, C. Baumann, F. Lang, A.E. Busch, H. Koepsell, Cloning and characterization of two human polyspecific organic cation transporters, DNA Cell Biol. 16 (1997) 871–881.

[11] R. Kerb, U. Brinkmann, N. Chatskaia, D. Gorbunov, V. Gorboulev, E. Mornhinweg, A. Keil, M. Eichelbaum, H. Koepsell, Identification of genetic variations of the human organic cation transporter hOCT1 and their functional consequences, Pharmacogenetics 12 (2002) 591–595.

[12] Y. Shu, M.K. Leabman, B. Feng, L.M. Mangravite, C.C. Huang, D. Stryke, M. Kawamoto, S.J. Johns, J. DeYoung, E. Carlson, T.E. Ferrin, I. Herskowitz, K.M. Giacomini, Pharmacogeneticis of membrane transporters investigators, evolutionary conservation predicts function of variants of the human organic cation transporter, OCT1, Proc. Natl. Acad. Sci. 100 (2003) 5902–5907.

[13] M. Hirakawa, T. Tanaka, Y. Hashimoto, M. Kuroda, T. Takagi, Y. Nakamura, JSNP: a database of common gene variations in the Japanese population, Nucleic Acids Res. 30 (2002) 158–162.

[14] H. Kusuhara, T. Sekine, N. Utsunomiya-Tate, M. Tsuda, R. Kojima, S.H. Cha, Y. Sugiyama, Y. Kanai, H. Endou, Molecular cloning and characterization of a new multispecific organic anion transporter from rat brain, J. Biol. Chem. 274 (1999) 13675–13680.

[15] G. Burckhardt, N.A. Wolff, Strucutre of renal organic anion and cation transporters, Am. J. Physiol. Renal Physiol. 278 (2000) F853–F866.

[16] R. Granthan, Amino acid difference formula to help explain protein evolution, Science 185 (1974) 862–864.

[17] S. Henikoff, J.G. Henikoff, Amino acid substitution matrices from protein blocks, Proc. Natl. Acad. Sci. USA 89 (1992) 10915–10919.

[18] J.W. Jonker, E. Wagenaar, C.A.A.M. Mol, M. Buitelaar, H. Koersell, J.W. Smit, A.H. Schinkel, Reduced hepatic uptake and intestinal excretion of organic cations in mice with a targeted disruption of the organic cation transporter 1 (*Oct1* [*Slc22a1*]) gene, Mol. Cell. Biol. 21 (2001) 5471–5477.

[19] D.-S. Wang, J.W. Jonker, Y. Kato, H. Kusuhara, A.H. Shinkel, Y. Sugiyama, Involvement of organic cation transporter 1 in hepatic and intestinal distribution of metformin, J. Pharmacol. Exp. Ther. 302 (2002) 510–515.

[20] J.F. Wilson, M.E. Weale, A.C. Smith, F. Gratrix, B. Fletcher, M.G. Thomas, N. Bladman, D.B. Goldstein, Population genetic structure of variable drug response, Nat. Genet. 29 (2001) 265–269.

[21] K. Okumura, T. Kita, S. Chikazawa, F. Komada, S. Iwakawa, Y. Tanigawara, Genotyping of *N*-acetylation polymorphism and correlation with procainamide metabolism, Clin. Pharmacol. Ther. 61 (1997) 509–517.

[22] R.L. Woosley, D.E. Drayer, M.M. Reidenberg, A.S. Nies, K. Carr, J.A. Oates, Effect of acetylator phenotype on the rate at which procainamide induces antinuclear antibodies and the lupus syndrome, N. Eng. J. Med. 298 (1978) 1157–1159.

[23] X. Jiang, G. Khursigara, R.L. Rubin, Transformation of lupus-inducing drugs to cytotoxic products by activated neutrophils, Science 266 (1994) 810–813.

J Pharmacol Sci 94, 297 – 304 (2004)

Journal of Pharmacological Sciences

Full Paper

Human Organic Anion Transporter 4 Is a Renal Apical Organic Anion/Dicarboxylate Exchanger in the Proximal Tubules

Sophapun Ekaratanawong[1,2], Naohiko Anzai[1], Promsuk Jutabha[1], Hiroki Miyazaki[1], Rie Noshiro[1], Michio Takeda[1], Yoshikatsu Kanai[1], Samaisukh Sophasan[3], and Hitoshi Endou[1,*]

[1]*Department of Pharmacology and Toxicology, Kyorin University School of Medicine, 6-20-2 Shinkawa, Mitaka, Tokyo 181-8611, Japan*
[2]*Department of Preclinical Sciences, Faculty of Medicine, Thammasat University, Klong Luang Pathumthani 12121, Thailand*
[3]*Department of Physiology, Faculty of Science, Mahidol University, Bangkok 10400, Thailand*

Received December 25, 2003; Accepted January 8, 2004

Abstract. Human organic anion transporter OAT4 is expressed in the kidney and placenta and mediates high-affinity transport of estrone-3-sulfate (E_1S). Because a previous study demonstrated no *trans*-stimulatory effects by E_1S, the mode of organic anion transport via OAT4 remains still unclear. In the present study, we examined the driving force of OAT4 using mouse proximal tubular cells stably expressing OAT4 (S_2 OAT4). OAT4-mediated E_1S uptake was inhibited by glutarate (GA) (IC_{50}: 1.25 mM) and [^{14}C]GA uptake via S_2 OAT4 was significantly *trans*-stimulated by unlabeled GA (5 mM) ($P<0.001$). [^{3}H]E_1S uptake via S_2 OAT4 was significantly *trans*-stimulated by preloaded GA ($P<0.001$) and its [^{14}C]GA efflux was significantly *trans*-stimulated by unlabeled E_1S in the medium ($P<0.05$). In additon, both the uptake and efflux of [^{14}C]*p*-aminohippuric acid (PAH) and [^{14}C]GA via S_2 OAT4 were significantly *trans*-stimulated by unlabeled GA or PAH. The immunoreactivities of OAT4 were observed in the apical membrane of proximal tubules along with those of basolateral organic anion/dicarboxylate exchangers such as hOAT1 and hOAT3 in the same tubular population. These results indicate that OAT4 is an apical organic anion/dicarboxylate exchanger and mainly functions as an apical pathway for the reabsorption of some organic anions in renal proximal tubules driven by an outwardly directed dicarboxylate gradient.

Keywords: organic anion, dicarboxylate, proximal tubule, organic anion transporter

Introduction

The kidney plays an important role in the elimination of harmful endogenous compounds and xenobiotics from the body. The proximal tubule is the primary site where numerous organic anions are taken up from the blood and excreted into the urine. (1, 2). The transcellular secretion of organic anion in the proximal tubule involves a two-step process: an uptake across the basolateral membrane of proximal tubular cells and an exit across the apical membrane into the tubular lumen. The former is energetically uphill and is accomplished by a tertiary active process via the organic anion/dicarboxylate exchanger that uses outwardly directed gradient of dicarboxylates such as α-ketoglutarate (3, 4). The latter is believed to be transporter-mediated, although this process is energetically downhill. In general, the efflux system for *p*-aminohippuric acid (PAH) (a prototypical substrate for the organic anion transport system) in the brush-border (apical) membrane has been investigated using brush-border membrane vesicles (BBMVs) (2). The existence of at least two transport systems was reported in human BBMVs, that is, a potential-driven facilitated diffusion and an organic anion/dicarboxylate exchange mechanism. To date, the mechanism of an apical organic anion exit pathway remains still uncertain.

Recently, several cDNAs encoding organic anion transporter have been successively identified in the

*Corresponding author. FAX: +81-422-79-1321
E-mail: endouh@kyorin-u.ac.jp

kidney, including organic anion transporter (OAT), organic anion transporting polypeptide (oatp), multidrug resistance-associated protein (MRP), and sodium-dependent inorganic phosphate transporter (NPT) families (3, 5, 6). Until now, it has been clarified that OAT1 and OAT3 are the PAH/dicarboxylate exchangers located at the basolateral membrane of proximal tubules (7 – 12). Rodent organic anion transporters, such as oatp1 and Oat-K1/K2, are located in the apical membrane of proximal tubules, but their homologues in humans have not yet been identified (3, 5, 6). Oatp5, a novel member of the oatp family in rodents, was cloned and shown to be expressed only in the kidney. However, its localization and functional characteristics have not yet been identified (13). In humans, MRP2 and NPT1, which are also localized in the apical membrane of proximal tubules (14 – 16), show PAH transport (K_m: 0.88 – 1.9 mM for MRP2; K_m: 2.66 mM for NPT1), although the relative contributions of both transporters to its apical exit are yet to be identified. Very recently, we have identified a novel voltage-driven organic anion transporter (OAT_V1) at the apical membrane of pig renal proximal tubules (17). OAT_V1 seems to be a long-hypothesized potential-driven facilitator in pig BBMVs (18). OAT_V1 exhibited the highest amino acid sequence identity to NPT1 (60 – 65%), although the functional properties of both transporters are different. Therefore, it needs to be elucidated whether OAT_V1 is an orthologue of human NPT1, but it is suggested that NPT1 is a good candidate for the apical potential-driven facilitator in human proximal tubules characterized in earlier experiments on BBMVs (2).

As previously reported, OAT4 is exclusively expressed in the human kidney and placenta, mediates the high-affinity transport of estrone-3-sulfate (E_1S) (K_m = 1.01 μM) and dehydroepiandrosterone sulfate (DHEAS) (K_m = 0.63 μM) (19), and is located in the apical membrane of renal proximal tubules (20). Although the apical membrane localization of OAT4 proposes its potential role in the organic anion secretion, its physiological importance in the kidney is still unclear due to the lack of information regarding its mode of transport. In the present study, we reinvestigated the driving force of OAT4. We report that OAT4 is not a facilitated transporter but an organic anion/dicarboxylate exchanger and mediate bidirectional organic anion transport. Furthermore, OAT4 is localized in the same population of hOAT1- and hOAT3-positive proximal tubular cells. These results indicate that OAT4 is a renal apical organic anion/dicarboxylate exchanger and mainly serves as a tubular reabsorptive pathway for some organic anions including sulfate conjugates driven by an outwardly directed gradient of dicarboxylates such as α-ketoglutarate.

Materials and Methods

Materials

The materials used here were purchased from the following sources: [^{14}C]PAH (1.90 GBq/mmol) and [^{3}H]E_1S (1.61 TBq/mmol) were from PerkinElmer Life Science Products (Boston, MA, USA); [^{14}C]glutarate (GA) (4.07 GBq/mmol) was from American Radiolabeled Chemicals, Inc. (St. Louis, MO, USA); GA was from Wako (Osaka). All other chemicals and reagents used were of analytical grade and obtained from commercial sources.

Cell culture and establishment of S_2 OAT4

The second segment of proximal tubules (S_2) cells, derived from transgenic mice harboring the temperature-sensitive simian virus 40 large T-antigen gene, were established as described previously (21). The establishments of S_2 OAT4 was reported previously (20, 22). These cells were grown in a humidified incubator at 33°C and under 5% CO_2 using RITC 80-7 medium containing 5% fetal bovine serum, 10 μg/ml transferrin, 0.08 U/ml insulin, 10 ng/ml recombinant epidermal growth factor, and 400 μg/ml geneticin. The cells were subcultured in a medium containing 0.05% trypsin-EDTA solution (137 mM NaCl, 5.4 mM KCl, 5.5 mM glucose, 4 mM $NaHCO_3$, 0.5 mM EDTA, and 5 mM HEPES, pH 7.2) and used for 25 to 35 passages.

Uptake study

Uptake experiments were performed as previously described (23). Organic anion transport in S_2 OAT4 was estimated by measuring the uptakes of [^{3}H]E_1S, [^{14}C]PAH, and [^{14}C]GA. S_2 OAT4 or S_2 pcDNA 3.1(+) (1×10^5 cells) was plated in 24-well plates and cultured for two days. After the medium was removed, the cell monolayers were washed twice with Dulbecco's modified phosphate-buffered saline (D-PBS) (137 mM NaCl, 3 mM KCl, 8 mM Na_2HPO_4, 1 mM KH_2PO_4, 1 mM $CaCl_2$, and 0.5 mM $MgCl_2$, pH 7.4) supplemented with 5.5 mM D-glucose and preincubated for 10 min. Then the monolayer was incubated with 500 μl of D-PBS containing 50 nM [^{3}H]E_1S, 20 μM [^{14}C]PAH or 10 μM [^{14}C]GA for 2 min (5 min for GA) at 37°C. Cells were washed three times with the ice cold D-PBS and solubilized in 0.5 ml of 0.1 N sodium hydroxide. The amount of substrate accumulated within the cells was then determined by measuring radioactivity.

Inhibition study

To evaluate the inhibitory effect of GA on E_1S uptake

mediated by OAT4, the cells were incubated in a medium containing [^{3}H]E_1S (50 nM) for 2 min in the absence or presence of various concentrations of GA at 37°C.

Examination of trans-stimulatory effect on the organic anion transport via OAT4

In order to clarify the driving force and its transport direction, we examined the *trans*-stimulatory effect on OAT4-mediated organic anion transport. For the uptake of radiolabeled substrates, the cells were prepared as described above, and the cells were preloaded with 0.5 ml of D-PBS with or without unlabeled substrates (E_1S, PAH, or GA; 5 mM each) at 37°C for 15 min before the uptake experiments. For the efflux of radiolabeled substrates, S_2 OAT4 and mock cells were seeded in 6-well tissue culture plates at a density of 4×10^5 cells/well. The cells were preloaded with 1 ml of D-PBS containing [^{3}H]E_1S (50 nM), [^{14}C]PAH (20 μM), or [^{14}C]GA (10 μM) at 37°C for 15 min, respectively. Then the cells were incubated in a medium with or without unlabeled substrates (GA and E_1S, PAH). Their radioactivities in the medium and that remaining in the cells were determined after 1-min (E_1S and PAH) or 5-min (GA) incubation.

Immunohistochemical analysis

The antibodies against hOAT1, hOAT3, and OAT4 used in this study have been shown to be specific for each protein, as previously described (11, 20, 24). We used human single-tissue slides (Biochain) for light microscopic immunohistochemical analysis using the streptavidin-biotin-HRP complex technique (LSAB kit; DAKO, Carpinteria, CA, USA). Sections were deparaffinized, rehydrated, and incubated with 3% H_2O_2 for 10 min to abrogate endogenous peroxidase activity. After rinsing in 0.05 M Tris-buffered saline containing 0.1% Tween 20 (TBST), the sections were treated with 10 μg/ml primary rabbit polyclonal antibodies (4°C overnight). Then the sections were incubated with the secondary antibody, biotinylated goat polyclonal antibody against rabbit immunoglobulin (DAKO), diluted 1:400, for 30 min with HRP-labeled streptavidin. This step was followed by incubation with diaminobenzidine and hydrogen peroxide. The sections were counterstained with hematoxylin and examined by light microscopy.

Statistical analyses

Data are expressed as the mean ± S.E.M. Statistical differences were determined by Student's *t*-test. The reproducibility of the results in the present study was confirmed using two or three separate experiments. The results from the representative experiments are shown in the figures.

Results

In our previous study, we reported that OAT4-mediated E_1S uptake is sodium-independent and not inhibited by 500 μM GA (a non-metabolized dicarboxylate) nor *trans*-stimulated by unlabeled E_1S (0.2 and 2 μM) (19). However, very recently, Sweet et al. and Bakhiya et al. showed that OAT3, which is considered to be a facilitated-diffusion carrier, is an organic anion/dicarboxylate exchanger similar to OAT1 (10, 12). Therefore, to test the interaction of GA with OAT4, we carried out *cis*-inhibition of OAT4-mediated E_1S uptake by GA at first.

As shown in Fig. 1A, E_1S uptake by OAT4 was largely inhibited by GA in millimolar concentrations (IC_{50}: 1.25 mM). This low-affinity seems to indicate the lack of inhibitory effect by 500 μM GA on OAT4-mediated E_1S transport in our previous work (19). Next, to test whether OAT4 transports GA, we performed a GA uptake study as well as the *trans*-stimulation experiment (Fig. 1B). For a 5-min incubation, the [^{14}C]GA uptake via OAT4 was twofold higher than that by mock cells ($P<0.01$). In addition, [^{14}C]GA uptake via OAT4 is *trans*-stimulated by preloaded GA (5 mM) ($P<0.001$), not by 1 mM GA. Then, to determine whether OAT4 is an organic anion/dicarboxylate exchanger, we tested the *trans*-stimulatory effect on the uptake and efflux of radiolabeled organic anion substrates via OAT4.

First, we used E_1S, an endogenous sulfate conjugate of steroid that is known to be a prototypical substrate for OAT4. The uptake of [^{3}H]E_1S was significantly *trans*-stimulated by preloaded GA (5 mM) (Fig. 2A), and the efflux of preloaded [^{14}C]GA was significantly stimulated with unlabelled E_1S in the medium (5 mM) (Fig. 2B). On the other hand, the uptake of [^{14}C]GA was not *trans*-stimulated by preloaded E_1S and the efflux of preloaded [^{3}H]E_1S was not stimulated with unlabelled GA in the medium (5 mM) (data not shown).

Then we used PAH, the prototypical xenobiotic substrate for renal organic anion transport. The uptake of [^{14}C]PAH was significantly *trans*-stimulated by preloaded GA (Fig. 3A) and the efflux of preloaded [^{14}C]GA was significantly stimulated with unlabelled PAH (5 mM) (Fig. 3B). In contrast to E_1S, the uptake of [^{14}C]GA was significantly *trans*-stimulated by preloaded PAH (Fig. 4A) and the efflux of preloaded [^{14}C]PAH was significantly stimulated with unlabelled GA in the medium (5 mM) (Fig. 4B). Similar *trans*-stimulatory effects were also observed in S_2 hOAT1 and S_2 hOAT3

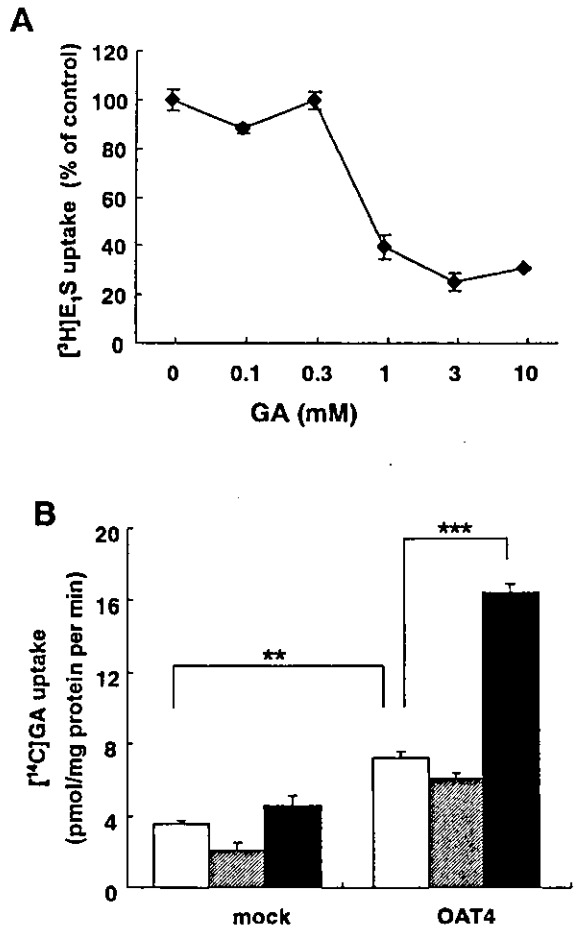

Fig. 1. Interaction of glutarate (GA) with OAT4. A: Inhibitory effect of GA on OAT4-mediated uptake of [^{3}H]E_1S. S_2 OAT4 cells were incubated in a solution containing 50 nM [^{3}H]E_1S at 37°C for 2 min in the absence or presence of various concentrations of GA at 37°C. B: OAT4-mediated [^{14}C]GA uptake. S_2 OAT4 cells and mock cells were preloaded with 0.5 ml of D-PBS with 0 mM (open column), 1 mM (hatched column), or 5 mM (solid column) of unlabeled GA at 37°C for 15 min before uptake experiments. Then they were incubated in a solution containing 10 μM [^{14}C]GA at 37°C for 5 min. Each value represents the mean ± S.E.M. of four determinations from one typical experiment of the two or three separate ones. $^{**}P<0.01$, $^{***}P<0.001$.

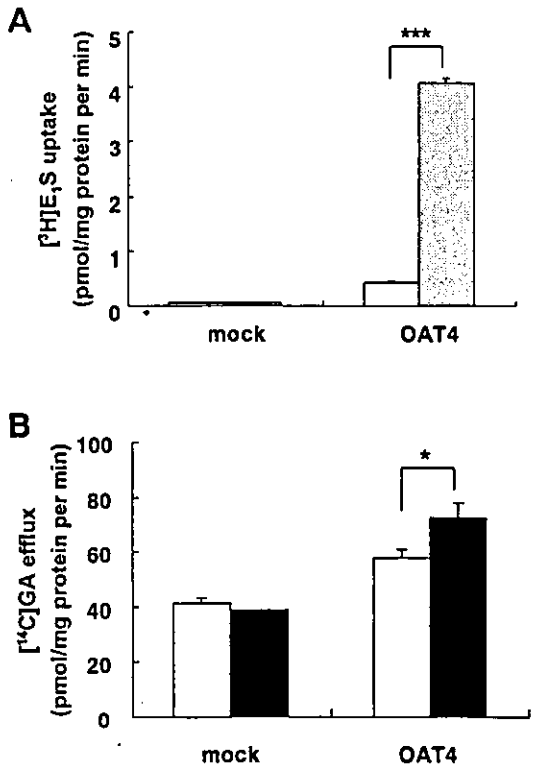

Fig. 2. *Trans*-stimulatory experiments regarding OAT4-mediated [^{3}H]E_1S uptake. A: *Trans*-stimulatory effect on the uptake of [^{3}H]E_1S by preloaded GA (5 mM). S_2 OAT4 cells and mock cells were preloaded with D-PBS in the absence (open column) or the presence of unlabeled GA (dotted column) at 37°C for 15 min before uptake experiments. The uptake rates of [^{3}H]E_1S by mock and S_2 OAT4 cells for 2 min were measured. B: *Trans*-stimulatory effect on the efflux of preloaded [^{14}C]GA by extracellular E_1S (5 mM). S_2 OAT4 cells and mock cells were preloaded with D-PBS in a solution containing 10 μM [^{14}C]GA at 37°C for 15 min before efflux experiments. The efflux rates of [^{14}C]GA by mock and S_2 OAT4 cells for 5 min were measured with (solid column) or without outside unlabeled E_1S (open column). Each value represents the mean ± S.E.M. of three or four determinations from one typical experiment of the three separate ones. $^*P<0.05$, $^{***}P<0.001$.

cells with 1 mM unlabeled compounds (data not shown).

To determine whether the apical organic anion /dicarboxylate exchanger (OAT4) is co-expressed along with basolateral organic anion/dicarboxylate exchanger (hOAT1 and hOAT3) in the same proximal tubules, we performed immunohistochemical analysis using serial sections of a human kidney (Fig. 5). The IgG fractions of rabbit polyclonal antibodies against the carboxyl termini of hOAT1, hOAT3, and OAT4 were used. The specificity of these antibodies was already reported previously (11, 20, 24). Light microscopy of 2-μm-thick paraffinized serial sections demonstrated that there is specific immunostaining of all three transporters in proximal tubular cells. At a high magnification, OAT4 localized in the apical membrane of proximal tubules (Fig. 5: E and F) along with hOAT1 (Fig. 5: A and B) and hOAT3 (Fig. 5: C and D) proteins expressed in the basolateral membrane of the same tubular cells.

Discussion

OAT4 was isolated from the human kidney cDNA library. When expressed in *Xenopus laevis* oocytes, OAT4 mediated the uptake of various substrates including E_1S, DHEAS, and PAH (19). The recent finding that OAT4 is localized at the apical membrane of proximal tubules suggested its role as an exit pathway

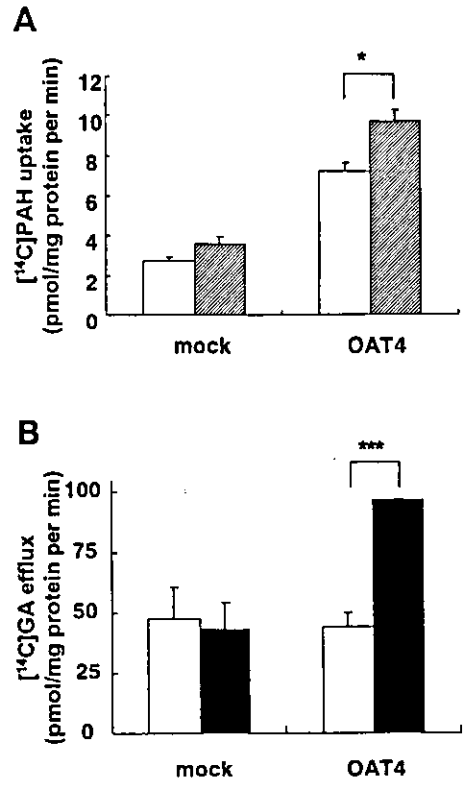

Fig. 3. *Trans*-stimulatory experiments regarding OAT4-mediated [^{14}C]PAH uptake. A: *trans*-stimulatory effect on the uptake of [^{14}C]PAH by preloaded GA (5 mM). S_2 OAT4 cells and mock cells were preloaded with D-PBS in the absence (open column) or the presence of unlabeled GA (hatched column) at 37°C for 15 min before uptake experiments. The uptake rates of [^{14}C]PAH by mock and S_2 OAT4 cells for 2 min were measured. B: *Trans*-stimulatory effect on the efflux of preloaded [^{14}C]GA by extracellular PAH (5 mM). S_2 OAT4 cells and mock cells were preloaded with D-PBS in a solution containing 10 μM [^{14}C]GA at 37°C for 15 min before efflux experiments. The efflux rates of [^{14}C]GA by mock and S_2 OAT4 cells for 5 min were measured with (solid column) or without outside unlabeled PAH (open column). Each value represents the mean ± S.E.M. of three or four determinations from one typical experiment of the three separate ones. *P<0.05, ***P<0.001.

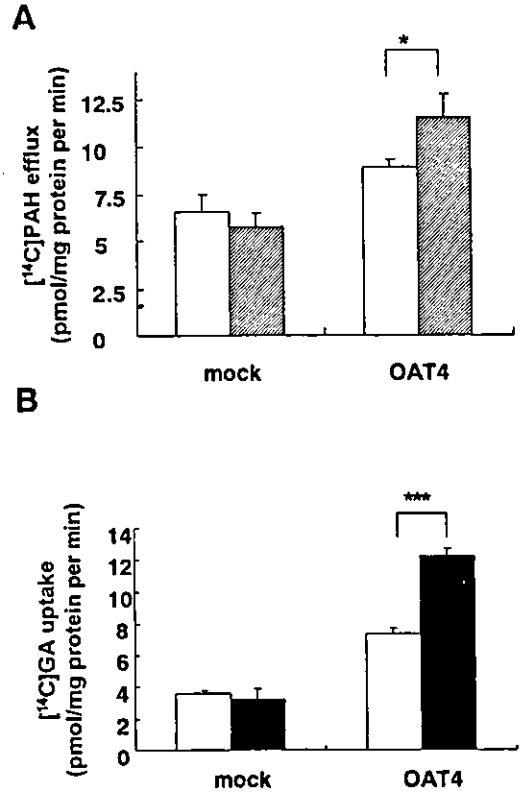

Fig. 4. *Trans*-stimulatory experiments regarding OAT4-mediated [^{14}C]PAH efflux. A: *trans*-stimulatory effect on the efflux of preloaded [^{14}C]PAH by extracellular GA (5 mM). S_2 OAT4 cells and mock cells were preloaded with D-PBS in a solution containing 20 μM [^{14}C]PAH at 37°C for 15 min before efflux experiments. The efflux rates of [^{14}C]PAH by mock and S_2 OAT4 cells for 1 min were measured with (hatched column) or without outside unlabeled GA (open column). B: *Trans*-stimulatory effect on the uptake of [^{14}C]GA by preloaded PAH (5 mM). S_2 OAT4 cells and mock cells were preloaded with D-PBS in the absence (open column) or the presence of unlabeled PAH (solid column) at 37°C for 15 min before uptake experiments. The uptake rates of [^{14}C]GA by mock and S_2 OAT4 cells for 5 min were measured. Each value represents the mean ± S.E.M. of four determinations from one typical experiment of the three separate ones. *P<0.05, ***P<0.001.

for organic anion (20). In the present study, we examined the properties of OAT4 as an apical organic anion /dicarboxylate exchanger.

This is the first report regarding the transport direction and the driving force of OAT4. Our data derived from stable OAT4-expressing cell lines from the S_2 segment of the mouse renal proximal tubule (S_2 OAT4) demonstrated that OAT4 functions as an organic anion /dicarboxylate exchanger. We used GA as a model compound for dicarboxylates in this study because GA is a non-metabolized dicarboxylate and exhibited the similar inhibitory potency on OAT4-mediated E_1S transport to α-ketoglutarate, physiologically the most abundant endogenous dicarboxylate in the proximal tubular cells (data not shown). The uptakes of [^{14}C]GA, [^{3}H]E_1S, and [^{14}C]PAH via S_2 OAT4 were significantly increased by the preincubation of unlabeled GA (Figs. 2A and 3A), and the [^{14}C]GA efflux was also significantly increased by the incubation with unlabeled E_1S or PAH (Figs. 2B and 3B). These results indicate that intracellular GA not only binds to OAT4 and *trans*-stimulates its organic anion uptake but also is translocated to the outside. Furthermore, the findings that [^{14}C]GA uptake via S_2 OAT4 was significantly increased by the preincubation of unlabeled PAH (Fig. 4B) and [^{14}C]PAH efflux was significantly increased by the incubation with unlabeled PAH (Fig. 4A) manifested the bidirectional transport characteristic of OAT4. These results raise the possibility that OAT4 is the organic anion/dicarboxylate exchange mechanism

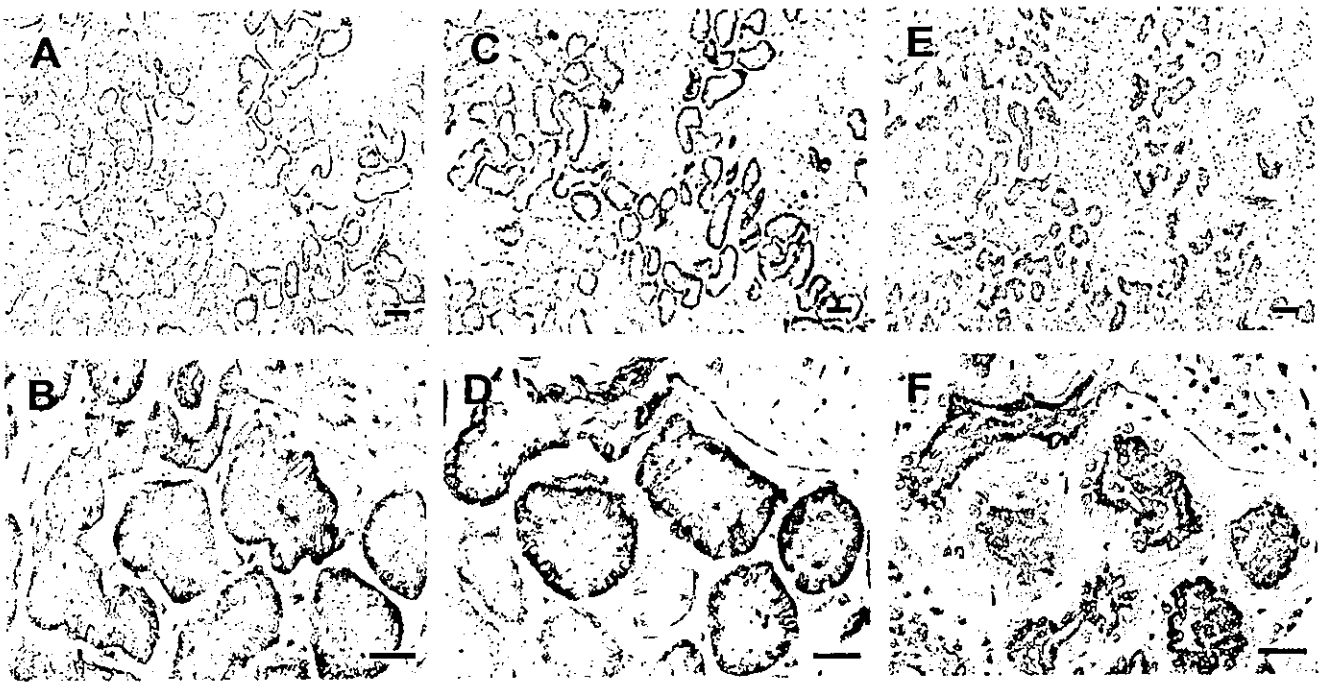

Fig. 5. Immunohistochemical analysis of human kidney. Two-micrometer serial sections were incubated with a polyclonal antibody against hOAT1, hOAT3, and OAT4. The apical membrane of proximal tubules was stained by OAT4 (E and F) and the same tubules showed basolateral membrane stained by both hOAT1 (A and B) and hOAT3 (C and D). (A, C, and E, 100×; B, D, and F, 400×). Scale bars = 100 μm for A, C, and E; 20 μm for B, D, and F.

previously found in BBMVs from human kidney (25).

As demonstrated in Fig. 5, now it became apparent that organic anion/dicarboxylate exchangers exist at both the apical (OAT4) and basolateral (OAT1 and OAT3) membrane of the same proximal tubular cells. As Schmitt and Burckhardt dicussed in the case of bovine BBMVs (26), it seems unlikely that two exchangers of the same type existing in both sides of membranes lead to the vectorial transport of organic anions. At the basolateral side of proximal tubules, it is widely accepted that the outwardly directed gradient of α-ketoglutarate, the most abundant dicarboxylate within proximal tubular cells, drives organic anion uptake. In contrast, little is known about the coupling between the dicarboxylate gradient and the anion exchange system, but taking the existence of the outwardly directed dicarboxylate gradient in the tubular cells into account, OAT4 seems to contribute to the tubular reabsorption of organic anions. One possible role of OAT4 is an apical backflux pathway (27) for some organic anions coupling to the apical organic anion efflux transporters such as MRP2, NPT1, and possibly, the human homologue of OAT$_V$1 (3, 5, 6, 17), as well as to the apical low affinity Na^+/dicarboxylate cotransporter NaDC-1 (28). Because the transport mode of these transporters is normally unidirectional, the stimulation or the inhibition of bidirectional OAT4 transport function may influence the net transepithelial secretion

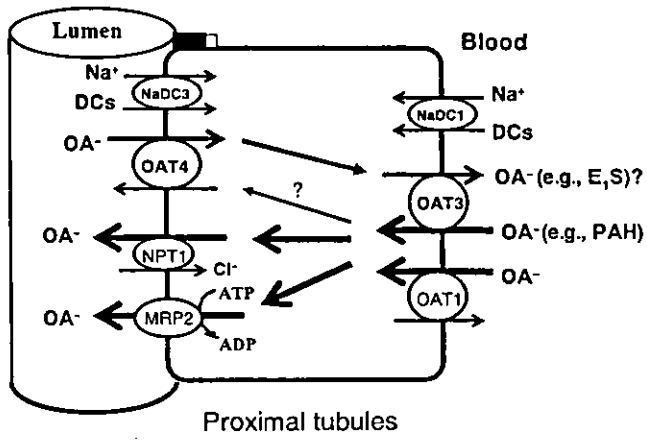

Fig. 6. Proposed model of transepithelial transport pathway for organic anions in human kidney. Organic anions including xenobiotics (e.g., PAH) enter into the proximal tubular cells via basolateral OAT1 and OAT3, and they are secreted into urine via apical MRP2 and NPT1, and in some cases, via OAT4. In contrast, endogenous organic anions such as E_1S and DHEAS reabsorbed via OAT4 may be effluxed via basolateral OAT3 or an unidentified transporter(s). Some organic anions may be reabsorbed from tubular lumen via OAT4 and may function as a backflux pathway. Abbreviations, OA: organic anion, DCs: dicarboxylates.

rate for organic anions. Recently, we have identified the intracellular interacting protein that regulates the OAT4-mediated transport function by the yeast two-hybrid assay (H. Miyazaki et al., manuscript in preparation). The functional coupling among apical transporters via intracellular protein(s) needs to be further clarified. Moreover, the substrate specificity of OAT4, which favors sulfate conjugates, is rather narrower than that of MRP2, NPT1, and OAT_V1. Therefore, another possibility is that OAT4 may contribute to avoid losing endogenous sulfated conjugates of steroid such as E_1S and DHEAS, which are the reservoir of steroids in the blood circulation (29, 30). These steroids are known to be tubular reabsorbed (31, 32). In this case, OAT3 may be a basolateral efflux pathway for sulfate conjugates of steroids. A proposed model of the transepithelial transport pathway for organic anions in human kidney is shown in Fig. 6.

Although OAT4 is expected to drive the uptake of organic anions into the cells, it is still uncertain whether OAT4 functions as an exit pathway for organic anions because it is not evident whether dicaboxylate concentrations in the cytoplasm are homogenous throughout tubular cells. The fact that the dicaboxylate is the counterion of OAT4 suggests that the directions of organic anion transport via OAT4 depend on the local concentration gradient of dicarboxylates across the plasma membrane, but there is no precise report regarding the efficiency or the contribution of the apical dicarboxylate gradient. In addition, in some pathological conditions, OAT4 may function as an apical exit pathway for organic anions because of its insensitivity to intracellular ATP content, Na^+ gradient, and membrane depolarization. For example, a mycotoxin, Ochratoxin A, produces alterations in renal function by inhibiting mitochondrial oxidation (33). Due to the mitochondrial damage, ATP production decreases, depolarization of the membrane potential occurs, and the Krebs-cycle reaction may be inhibited. In such a case, the bidirectional transport characteristic of OAT4 may contribute to the xenobiotics secretion into the urine in exchange for extracellular dicarboxylates regardless of ATP, Na^+, and membrane potential.

In this study, we observed no *trans*-stimulatory effect on E_1S efflux by outside GA and on GA uptake by preloaded E_1S from S_2 OAT4. A similar observation was reported by Bakhiya et al. in hOAT3-expressing oocytes (12). They explained that due to the high lipophilicity of E_1S, binding to intracellular components upon oocyte injection reduces the free submembraneous E_1S concentration available for efflux. This may not be true because, as we have reported recently, approximately 25% of injected E_1S is effluxed by the voltage-driven organic anion transporter OAT_V1 (17). Therefore, we propose another possibility that these findings relate to the difference of intracellular and extracellular side substrate binding sites. That is, OAT4 can recognize PAH from both intracellular and extracellular sides, but it can recognize E_1S only from the extracellular side. Further studies are necessary to clarify this problem.

The present findings with OAT4 raise the possibility that dicarboxylate exchange is a common mechanism for this family of transporters. It is well established that OAT1 is a classical PAH/dicarboxylate exchanger. In addition, two recent reports support our idea. First, Sweet et al. and Bakhiya et al. reported that OAT3 functions as an organic anion/dicarboxylate exchanger (10, 12). Second, we reported the cloning of a novel member of the OAT family, urate/anion exchanger 1 (URAT1) (34). URAT1 is expressed at the apical membrane of proximal tubules and it is thought to be the long-hypothesized urate/anion exchanger in the human kidney; however, the transport of PAH has not been observed. OAT4 exhibited the highest amino acid sequence identity to URAT1 and higher amino acid sequence identities to OAT1 and OAT3 among the OAT family. Particularly, all these clones (OAT4, OAT1, OAT3, and URAT1) have long intracellular loops (about 70 amino acids) that are thought to be a structural characteristic of antiporter (35). The fact that not only OAT1 and OAT3 but also URAT1 has an exchange mode seems to be appropriate for the OAT4 functions as an exchanger. Therefore it is interesting to know the common inherent structural traits responsible for such similar exchange mechanisms developed among different transporters. Further studies are needed to elucidate this possibility.

In conclusion, we first demonstrated that OAT4 is the bidirectional organic anion/dicarboxylate exchanger. OAT4 may function as an apical reabsorptive pathway of some organic anions in the proximal tubules under the physiological condition, but it may also drive the tubular secretion of organic anions in some conditions. Although the relative contribution of OAT4 in renal organic anion handling needs to be clarified, this study provides new insights into the functional basis of the transepithelial transport pathway of organic anions, including xenobiotics and endogenous compounds, in the human kidney.

Acknowledgments

This work was supported, in part, by grants from the Ministry of Education, Culture Sports, Science, and Technology of Japan; by grants from the Japanese Society for the Promotion of Science (JSPS); by

RONPAKU program of JSPS; and by Grants-in-Aids for Scientific Research and Bioventure Project from the Science Research Promotion Fund of the Japan Private School Promotion Foundation.

References

1 Moller JV, Sheikh MI. Renal organic anion transport system: pharmacological, physiological, and biochemical aspects. Pharmacol Rev. 1983;34:315–358.

2 Pritchard JB, Miller DS. Mechanism mediating renal secretion of organic anions and cations. Physiol Rev. 1993;73:765–796.

3 Burckhardt G, Bahn A, Wolff NA. Molecular physiology of renal *p*-aminohippurate secretion. New Physiol Sci. 2001;16: 114–118.

4 Sekine T, Cha SH, Endou H. The multispecific organic anion transporter (OAT) family. Pfluger Arch. 2000;440:337–350.

5 Inui KI, Masuda S, Saito H. Cellular and molecular aspects of drug transport in the kidney. Kidney Int. 2000;58:944–958.

6 Russel FGM, Masereeuw R, van Aubel RAMH. Molecular aspects of renal anionic drug transport. Annu Rev Physiol. 2002; 64:563–594.

7 Sekine T, Watanabe N, Hosoyamada M, Kanai Y, Endou H. Expression cloning and characterization of a novel multispecific organic anion transporter. J Biol Chem. 1997;272:18526–18529.

8 Sweet DH, Wolff NA, Pritchard JB. Expression cloning and characterization of ROAT1. The basolateral organic anion transporter in rat kidney. J Biol Chem. 1997;272:30088–30095.

9 Kusuhara H, Sekine T, Utsunomiya-Tate N, et al. Molecular cloning and characterization of a new multispecific organic anion transporter from rat brain. J Biol Chem. 1999;274:13675–13680.

10 Sweet DH, Chan LM, Walden R, Yang XP, Miller DS, Pritchard JB. Organic anion transporter 3 (Slc22a8) is a dicarboxylate exchanger indirectly coupled to the Na^+ gradient. Am J Physiol Renal Physiol. 2003;284:F763–F769.

11 Cha SH, Sekine T, Fukushima J, et al. Identification and characterization of human organic anion transporter 3 expressing predominantly in the kidney. Mol Pharmacol. 2001;59:1277–1286.

12 Bakhiya N, Bahn A, Burckhardt G, Wolff NA. Human organic anion transporter 3 (hOAT3) can operate as an exchanger and mediate secretory urate flux. Cell Physiol Biochem. 2003;13: 249–256.

13 Choudhuri S, Ogura K, Klaassen D. Cloning, expression, and ontogeny of mouse organic anion-transporting polypeptide-5, a kidney-specific organic anion transporter. Biochem Biophys Res Commun. 2001;280:92–98.

14 Leier I, Hummel-Eisenbeiss J, Chi Y, Keppler D. ATP-dependent *para*-aminohippurate transport by apical multidrug resistance protein MRP2. Kidney Int. 2000;57:1636–1642.

15 van Aubel RAMH, Peters JGP, Masereeuw R, van Os CH, Russel FGM. Multidrug resistance protein Mrp2 mediates ATP-dependent transport of classic renal organic anion *p*-aminohippurate. Am J Physiol Renal Physiol. 2000;279:F713–F717.

16 Uchino H, Tamai I, Yamashita K, et al. *p*-Aminohippuric acid transport at renal apical membrane mediated by human inorganic phosphate transporter NPT1. Biochem Biophys Res Commun. 2000;270:254–259.

17 Jutabha P, Kanai Y, Hosoyamada M, et al. Identification of a novel voltage-driven organic anion transporter present at apical membrane of renal proximal tubule. J Biol Chem. 2003;278: 27930–27938.

18 Werner D, Martinez F, Roch-Ramel F. Urate and *p*-aminohippurate transport in the brush border membrane of pig kidney. J Pharmacol Exp Ther. 1990;252:792–799.

19 Cha SH, Sekine T, Kusuhara H, et al. Molecular cloning and characterization of multispecific organic anion transporter 4 expressed in the placenta. J Biol Chem. 2000;275:4507–4512.

20 Babu E, Takeda M, Narikawa S, et al. Role of human organic anion transporter 4 in the transport of ochratoxin A. Biochim Biophys Acta. 2002;1590:64–75.

21 Hosoyamada M, Obinata M, Suzuki H, Endou H. Cisplatin-induced toxicity in immortalized renal cell lines established from transgenic mice harboring temperture sensitive SV40 large T-antigen gene. Arch Toxicol. 1996;70:282–292.

22 Takeda M, Khamdang S, Narikawa S, et al. Characterization of methotrexate transport and its drug interactions with human organic anion transporters. J Pharmacol Exp Ther. 2002;302: 666–671.

23 Takeda M, Tojo A, Sekine T, Hosoyamada M, Kanai Y, Endou H. Role of organic anion transporter 1 (OAT1) in cephaloridine-induced nephrotoxicity. Kidney Int. 1999;56:2128–2136.

24 Hosoyamada M, Sekine T, Kanai Y, Endou H. Molecular cloning and functional expression of a multispecific organic anion transporter from human kidney. Am J Physiol. 1999;276: F122–F128.

25 Roch-Ramel F, Guisan B, Schild L. Indirect coupling of urate and *p*-aminohippurate transport to sodium in human brush-border membrane vesicles. Am J Physiol Renal Physiol. 1996;270:F61–F68.

26 Schmitt C, Burckhardt G. *p*-Aminohippurate/2-oxoglutarate exchange in bovine renal brush-border and basolateral membrane vesicles. Pflugers Arch. 1993;423:280–290.

27 Dantzler WH. Renal organic anion transport: a comparative and cellular perspective. Biochim Biophys Acta. 2002;1566:169–181.

28 Pajor AM. Molecular properties of sodium/dicarboxylate cotransporters. J Membr Biol. 2000;175:1–8.

29 Loriaux DL, Ruder HJ, Lipsett MB. The measurement of estrone sulfate in plasma. Steroids. 1971;18:463–472.

30 Ebeling P, Koivisto VA. Physiological importance of dehydroepiandrosterone. Lancet. 1994;343:1479–1481.

31 Wright K, Collins DC, Musey PI, Preedy JRK. A specific radioimmunoassay for estrone sulfate in plasma and urine without hydrolysis. J Clin Endocrinol Metab. 1978;47:1092–1098.

32 Kellie AE, Smith ER. Renal clearance of 17-oxo steroid conjugates found in human peripheral plasma. Biochem J. 1957;66: 490–495.

33 Jung KY, Endou H. Nephrotoxicity assessment by measuring cellular ATP content. II. Intranephron site of ochratoxin A nephrotoxicity. Toxicol Appl Pharmacol. 1989;100:383–390.

34 Enomoto A, Kimura H, Chairoungdua A, et al. Molecular identification of a renal urate-anion exchanger that regulates blood urate levels. Nature. 2002;417:447–452.

35 Huang Y, Lemieux MJ, Song J, Auer M, Wang D-N. Structure and mechanism of the glycerol-3-phosphate transporter from *Escherichia coli*. Science. 2003;301:616–620.

Available online at www.sciencedirect.com
SCIENCE DIRECT
Cancer Letters 205 (2004) 215–226
CANCER Letters
www.elsevier.com/locate/canlet

Expression and functional characterization of the system L amino acid transporter in KB human oral epidermoid carcinoma cells

Jung Hoon Yoon[a], Youn Bae Kim[a], Myong Soo Kim[a], Joo Cheol Park[a], Joong Ki Kook[a], Hae Man Jung[a], Saeng Gon Kim[a], Hoon Yoo[a], Yeong Mu Ko[a], Sang Ho Lee[a], Bong Young Kim[b], Hong Sung Chun[c], Yoshikatsu Kanai[d], Hitoshi Endou[d], Do Kyung Kim[a,*]

[a]*Oral Biology Research Institute, Chosun University College of Dentistry, 375 Seosuk-dong, Dong-gu, Gwangju 501-759, South Korea*
[b]*Department of Pathology, Korea University College of Medicine, Seoul 136-705, South Korea*
[c]*Division of Biological Science, Chosun University, Gwangju 501-759, South Korea*
[d]*Department of Pharmacology and Toxicology, Kyorin University School of Medicine, 6-20-2 Shinkawa, Mitaka, Tokyo 181-8611, Japan*

Received 9 March 2003; received in revised form 2 September 2003; accepted 3 October 2003

Abstract

We have examined the expression and function of system L amino acid transporter in KB human oral epidermoid carcinoma cells. The KB cells express L-type amino acid transporter 1 (LAT1) in plasma membrane, but not L-type amino acid transporter 2 (LAT2). The [^{14}C]L-leucine uptake by KB cells is inhibited by system L selective inhibitor BCH. The majority of [^{14}C]L-leucine uptake is, therefore, mediated by LAT1. These results suggest that the transport of neutral amino acids including several essential amino acids into the KB cells mediated by LAT1 and the specific inhibition of LAT1 in oral cancer cells will be a new rationale for anti-cancer therapy.

Keywords: L-Type amino acid transporter; KB human oral epidermoid carcinoma cells; Essential amino acids; Anti-cancer therapy

1. Introduction

Amino acid is indispensable to support the protein synthesis required for cell growth and proliferation [1,2]. Amino acid transport across the plasma membrane is mediated via amino acid transporters located on the plasma membrane. Among the amino acid transport systems, system L amino acid transporter mediates Na^+-independent transports of large neutral amino acids including several essential amino acids [1,3]. It is a major route for providing living cells including tumor cells with branched or aromatic amino acids [1,3]. Because of its broad substrate selectivity, system L amino acid transporter

Abbreviations: LAT1, L-type amino acid transporter 1; LAT2, L-type amino acid transporter 2; 4F2hc, 4F2 heavy chain; BCH, 2-aminobicyclo-(2,2,1)-heptane-2-carboxylic acid.

* Corresponding author. Tel.: +82-62-230-6893; fax: +82-62-223-3205.
E-mail address: kdk@chosun.ac.kr (D.K. Kim).

0304-3835/$ - see front matter © 2003 Elsevier Ireland Ltd. All rights reserved.
doi:10.1016/j.canlet.2003.10.009